Journal of Physics: Conference Series **558** (2014) 012015 doi:10.1088/1742-6596/558/1/012015

Unconventional phases of the alternating-spin Heisenberg chain with extra three-body exchange terms

N B Ivanov[1,2] **and J Schnack**[1]

[1]Fakultät für Physik, Universität Bielefeld, Postfach 100131, D-33501 Bielefeld, Germany
[2]ISSP, Bulgarian Academy of Sciences, Tzarigradsko chaussee 72, 1784 Sofia, Bulgaria

E-mail: nedko.ivanov@physik.uni-magdeburg.de

Abstract. The Heisenberg chain with alternating site spins $(S, \sigma) = (1, \frac{1}{2})$ defines a realistic prototype model admitting extra isotropic three-body exchange terms which drive the chain into exotic quantum phases. In this paper, we focus on the non-magnetic part of the phase diagram. Based on numerical density-matrix renormalization group and exact-diagonalization calculations, we demonstrate that the nearest-neighbor three-body interaction stabilizes (i) a critical spin liquid phase described by two Gaussian conformal theories as well as (ii) a critical nematic-like phase characterized by dominant quadrupolar S-spin fluctuations. The emergence of these phases reflects some specific features of the three-body terms such as the promotion of local collinear spin configurations and the enhanced tendency towards nearest-neighbor clustering of the spins.

1. Introduction

Competing higher-order exchange interactions have been identified as an excellent source of exotic quantum effects and phases [1]. For instance, Heisenberg models with the additional two-site biquadratic terms $(\boldsymbol{S}_i \cdot \boldsymbol{S}_j)^2$ – such as the spin-1 bilinear-biquadratic chain [2] and its higher-dimensional counterparts on square [3, 4], triangular [5, 6], and cubic [3] lattices – constitute a class of widely discussed systems supporting rich phase diagrams.

In contrast, for the time being the role of the isotropic three-body exchange terms $(\boldsymbol{S}_i \cdot \boldsymbol{S}_j)(\boldsymbol{S}_i \cdot \boldsymbol{S}_k) + h.c.$ $(|\boldsymbol{S}_i| > \frac{1}{2}, i \neq j, k; j \neq k)$ remains scarcely explored. On the theoretical side, such terms have been primarily used as a tool for constructing various exactly-solvable one-dimensional (1D) models [7, 8, 9, 10]. Some special effects of the isotropic three-body exchange interactions in generic spin-S Heisenberg models have only recently been discussed [11, 12, 13, 14]. On the experimental side, more convincing experimental evidence for three-body exchange effects comes from inelastic neutron scattering measurements in the magnetic material $CsMn_xMg_{1-x}Br_3$ $(x = 0.28)$ [15], $CsMnBr_3$ being known as a nearly ideal spin-$\frac{5}{2}$ Heisenberg antiferromagnetic (AFM) chain. The experimental results imply nearly equal strengths of both the biquadratic and three-site terms, which are about two orders of magnitude weaker than the principal Heisenberg coupling. In this material, the emergence of effective higher-order exchange terms was attributed to the strong magenetoelastic forces [16]. Another source of three-body exchange interactions could be the two-orbital Hubbard model, where similar terms appear in the fourth order of the strong-coupling expansion [11].

In the discussed systems, that are dominated by the Heisenberg coupling, the strengths of both higher-order terms are controlled by one and the same model parameter, so that it might be a challenge to isolate the effects resulting from three-site terms. In this connection, cold atoms in optical lattices seem to offer a promising route. For instance, as demonstrated in Ref. [17], the two-species Bose-Hubbard model in a triangular configuration can be used to generate a wide range of Hamiltonian operators, including effective three-body interactions, resulting from atomic tunnelings through different lattice paths. A general purpose of this paper is to demonstrate that some conventional alternating-spin Heisenberg systems could provide another promising route [18]. We concentrate on a prototype 1D model of this class, admitting extra three-body exchange terms, defined by the Hamiltonian

$$\mathcal{H}_{\sigma S}=\sum_{n=1}^{L}h_n\equiv\sum_{n=1}^{L}J_1\boldsymbol{S}_{2n}\cdot(\boldsymbol{\sigma}_{2n-1}+\boldsymbol{\sigma}_{2n+1})+J_2\left[(\boldsymbol{S}_{2n}\cdot\boldsymbol{\sigma}_{2n-1})\,(\boldsymbol{S}_{2n}\cdot\boldsymbol{\sigma}_{2n+1})+h.c.\right], \qquad (1)$$

where L stands for the number of elementary cells containing two different spins ($S>\sigma$). In what follows we use the standard parameterization of the coupling constants $J_1=\cos(t)$ and $J_2=\sin(t)$ $(0\leq t<2\pi)$.

In view of the numerous experimentally accessible quasi-1D spin systems described by the Heisenberg model with different pairs (S,σ) of alternating spins [19, 20, 21], the suggested model defines a simple but realistic onset to explore the impact of three-body exchange interactions. Note that for systems with $\sigma=\frac{1}{2}$ the biquadratic terms reduce to bilinear forms [22, 23, 24]. The following analysis, based on numerical density-matrix renormalization group (DMRG) and exact diagonalization (ED) calculations, is concentrated on the non-magnetic part of the ground-state (GS) phase diagram of $\mathcal{H}_{\sigma S}$ in the extreme quantum limit $(S,\sigma)=(1,\frac{1}{2})$. Keeping up to 500 states in the last (seventh) sweep ensures in most cases good convergences (up to the largest simulated system with $L=256$) under open boundary conditions (OBC), with a discarded weight of the order of 10^{-8} or better. A detailed description of the full GS phase diagram will be presented elsewhere [25].

2. Classical states

To start with, let us briefly discuss the classical phase diagram of Eq. (1) including – apart from the standard ferromagnetic (FM) and Néel-type ferrimagnetic (FiM) phases – a highly-degenerate phase (D). These phases can be constructed from the three-spin GS configurations of the local Hamiltonians h_n. Indeed, suggesting $\boldsymbol{S}_{2n}=S(0,0,1)=\Uparrow$, one finds the GS cluster states $|\mathrm{FM}\rangle=\uparrow\Uparrow\uparrow$, $|\mathrm{FiM}\rangle=\downarrow\Uparrow\downarrow$, and $|\mathrm{D}\rangle_{L,R}=(\uparrow\Uparrow\downarrow,\downarrow\Uparrow\uparrow)$ respectively in the t intervals $(\frac{3\pi}{4},\frac{3\pi}{2})$, $(-\frac{\pi}{2},\frac{\pi}{4})$, and $(\frac{\pi}{4},\frac{3\pi}{4})$. Remarkably, apart from the boundary points $t=\frac{\pi}{4}$ and $\frac{3\pi}{4}$, the classical Hamiltonian h_n supports only collinear GS spin configurations. Now, by fitting the directions of the shared σ spins, we can use these cluster states as building blocks of global (L cell) spin configurations. By construction, the obtained states correspond to local minima of the classical energy. Obviously, for $t\in(\frac{3\pi}{4},\frac{3\pi}{2})$ $[t\in(-\frac{\pi}{2},\frac{\pi}{4})]$, the cluster state $|\mathrm{FM}\rangle$ ($|\mathrm{FiM}\rangle$) generates a unique global configuration representing the classical FM (FiM) phase. On the contrary, for $t\in(\frac{\pi}{4},\frac{3\pi}{4})$ there exists a manifold of degenerate optimal states based on the cluster states $|\mathrm{D}\rangle_{L,R}$ and their reversed-spin counterparts. As there are two ways to attach a new block to a given configuration, the degeneracy of the D phase is exponentially large (2^L). The established classical diagram was additionally confirmed by Monte Carlo simulations.

3. Critical spin-liquid phase (SL)

The DMRG analysis of the short-range (SR) correlations in open chains reveals in the interval $\frac{\pi}{6}\lesssim t\lesssim\frac{\pi}{2}$ a regular alternating-bond structure of the GS (and the lowest excited states) characterized by different values of the SR correlators $\langle\boldsymbol{\sigma}_{2n-1}\cdot\boldsymbol{S}_{2n}\rangle=u$ and $\langle\boldsymbol{S}_{2n}\cdot\boldsymbol{\sigma}_{2n+1}\rangle=v$

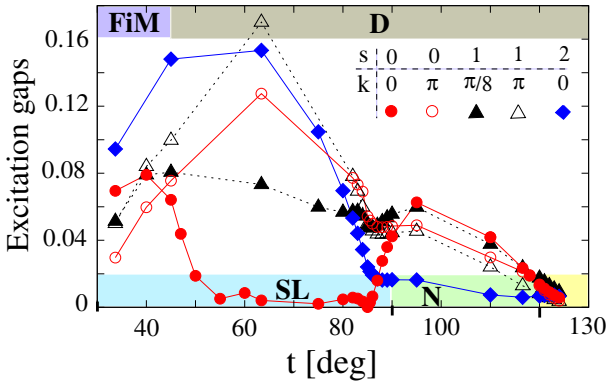

Figure 1. Numerical ED results (symbols) for the lowest excitation gaps in the $L = 8$ ring *vs* t. FiM and D are abbreviations for the ferrimagnetic (Néel type) and the 2^L-fold degenerate classical phases, respectively. SL and N denote, respectively, the spin liquid and nematic-like quantum phases discussed in the text. The lines are guides for the eye. Inset: Spins (s) and momenta (k) of the related excitations.

($u < v$). The uv (vu) "dimerized" GS $|\Psi_L\rangle$ ($|\Psi_R\rangle$) is stabilized in open chains with a σ spin on the left (right) end of the chain and corresponds to a uv (vu) dimerization of the local Hamiltonians h_n. The established uv structure of the GS is strongly pronounced in the middle of the SL region, where the values $(u, v) \approx (-1, \frac{1}{3})$ indicate the formation of nearly pure spin-$\frac{1}{2}$ states of the nearest-neighbor spins $\boldsymbol{S}_{2n} + \boldsymbol{\sigma}_{2n-1}$. Obviously, the established structural order does not violate the translational symmetry of the Hamiltonian $\mathcal{H}_{\sigma S}$ by two lattice sites.

Both types of alternating-bond states are related by the site parity operation $\mathcal{P}$: $\mathcal{P}|\Psi_{L,R}\rangle = |\Psi_{R,L}\rangle$. As the symmetry $\mathcal{P}$ is not violated in finite periodic chains, we may expect, in particular, two quasi-degenerate singlet states related to the combinations $|\Psi_\pm\rangle = \frac{1}{\sqrt{2}}(|\Psi_L\rangle \pm |\Psi_R\rangle)$. As seen in figure 1, a low-lying excited singlet state can be observed already in small rings ($L = 8$). A similar tendency towards doubling of the spectrum can also be identified for some triplet and quintet states in figure 2a. In fact, even in t regions with relatively large singlet gaps for small L – like the region around $t = 45°$ – the finite-size scaling (FSS) of the excitation gaps, figure 2b, supports this tendency: in particular, the FSS implies an exponentially fast (with L) doubling of the lowest singlet and triplet states. Due to strong boundary effects, the discussed doubling in the lowest part of the spectrum remains invisible in open chains up to the largest ($L = 256$) simulated system.

In figure 3a, we show DMRG results for the GS entanglement entropy $S(L, l)$ of the open alternating-spin chain at $t = 45°$. The analytical result for this quantity in critical conformally-invariant 1D systems reads [26, 27]

$$S(L, l) = \frac{c}{3\eta} \ln \left[\frac{\eta L}{\pi} \sin \left(\frac{\pi l}{L} \right) \right] + \text{const.} \qquad (2)$$

Here l is the number of unit cells in the subblock ($l = 1, \ldots, L$), c is the central charge, and $\eta = 1, 2$ for periodic boundary conditions (PBC) and OBC, respectively. The extrapolation of the numerical data for $S(L, L/2)$ *vs* $\ln(2L/\pi)$ up to $L = 256$ suggests a critical behavior with central charge $c = 1$, figure 3b. We observe two different branches of $S(L, l)$ corresponding to even and odd l. Similar even-odd oscillations have been originally reported in open spin-$\frac{1}{2}$ XXZ chains, including the isotropic limit [28]. In this work, it was clarified that the alternating part of $S(L, l)$, decaying away from the boundary with a universal power law, appears as a result of oscillations of the energy density. The latter oscillations were attributed to the tendency of

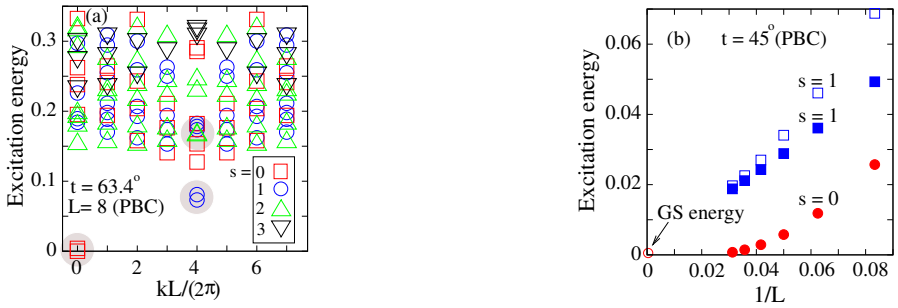

Figure 2. (a) Numerical ED results for the low-lying (spin $s = 0, 1, 2$, and 3) excitation energies of the periodic $L = 8$ chain at $t = 63.4°$. The shaded symbols correspond to the lowest quasi-degenerate pairs of singlet, triplet and quintet excitations. (b) DMRG results for the FSS of the lowest singlet and triplet modes at $t = 45°$.

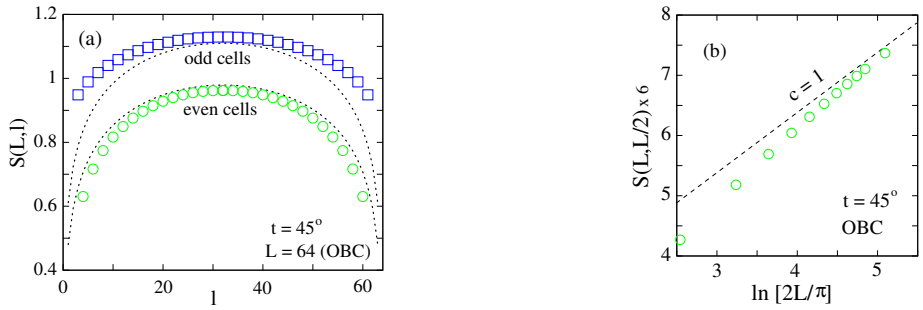

Figure 3. (a) Numerical DMRG results for the even- and odd-subblock GS entanglement entropy of the SL state ($t = 45°$) vs the number of subblock cells l. The dashed lines represent the theoretical result, Eq. (2), with $c = 1$. (b) Extrapolation of the DMRG results for $S(L, L/2)$ vs $\ln(2L/\pi)$ at $t = 45°$. The dashed line corresponds to $S(L, L/2)$ with the central charge $c = 1$.

the critical system towards formation of local singlet bonds, combined with the strong tendency of the end spins to form local singlets. To understand the even-odd cell modulation of $S(L, l)$ in the alternating spin chain, one can suggest a similar scenario, i.e., one may speculate that the even-odd cell modulation of $S(L, l)$ is related to the formation of local four-spin singlets. However, unlike for the XXZ chain, the formation of local singlet states in the alternating spin model is more complex as it includes, at least, four neighboring spins with two possible types of uv modulation.

Assuming conformal invariance, additional characteristic properties of the non-magnetic SL phase can be extracted from the FSS behavior of the GS and the lowest excited states. Numerical simulations of periodic chains are hampered by the quasi-degeneracy of the GS, so that the following analysis is performed under OBC. The expected tower of excited states related to some primary operator is defined by [29]

$$\Delta_n(L) \equiv E_n(L) - E_0(L) = \frac{\pi v_s}{L}(x_s + n) + o(L^{-1}), \tag{3}$$

where $n = 0, 1, 2, \ldots$. x_s is the universal surface exponent related to the same operator, and v_s is the sound velocity. The exponent x_s is known, in particular, for the energy states of the isotropic spin-$\frac{1}{2}$ Heisenberg chain in the m sectors ($x_s^{(m)} = m^2$, $m = 1, 2, \ldots$), where m is the z component of the total spin [30]. The Hamiltonian (1) respects the spin-rotation symmetry, so that the above asymptotic expression, when used as a fitting ansatz, has to be supplemented by

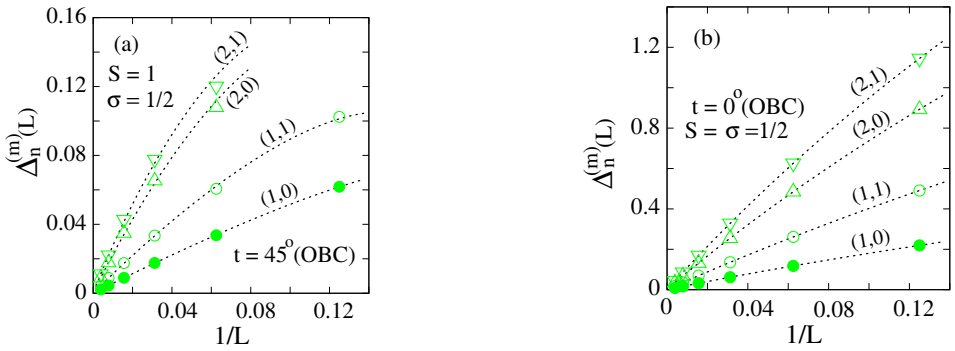

Figure 4. (a) FSS of the lowest triplet $[(m,n) = (1,0)$ and $(1,1)]$ and quintet $[(m,n) = (2,0)$ and $(2,1)]$ gaps in (a) the alternating spin $(1, \frac{1}{2})$ chain (DMRG, OBC, $t = 45°$) and (b) in the uniform $(\frac{1}{2}, \frac{1}{2})$ chain with $2L$ sites (DMRG, OBC, $t = 0°$). The dashed lines show the best fits to the DMRG data (symbols) obtained by Eq. (4).

appropriate logarithmic terms [31].

In figure 4, we compare FSS results for the lowest two excitations in the triplet $(m = 1)$ and quintet $(m = 2)$ towers of states of the Hamiltonian $\mathcal{H}_{\sigma S}$, Eq. (1), for two cases: (i) $(S,\sigma) = (1, \frac{1}{2})$ at $t = 45°$ and (ii) $(S,\sigma) = (\frac{1}{2}, \frac{1}{2})$ at $t = 0°$. The fit of the reduced gaps $L\Delta_n^{(m)}$ is performed by the four-parameter ansatz

$$L\Delta_n^{(m)}(L) = a_n^{(m)} + \frac{b_n^{(m)}}{\ln\left(L/\xi_n^{(m)}\right)} + \frac{c_n^{(m)}}{L}. \tag{4}$$

For systems belonging to the Gaussian universality class – like the isotropic spin-$\frac{1}{2}$ chain in the second case – the first fitting parameter $a_n^{(m)}$ is expected to approach the exact result $a_n^{(m)} = \pi v_s(m^2+n)/2$, which gives $[m,n] \equiv a_n^{(m)}/a_0^{(1)} = m^2 + n$. In fact, the performed fits for the $(S,\sigma) = (\frac{1}{2}, \frac{1}{2})$ chain give the numerical estimates [1,1]=1.99, [2,0]=3.99, and [2,1]=4.96, which excellently reproduce the expected theoretical ratios. Moreover, a comparison of Eqs. (3) and (4) implies the relation $a_0^{(1)} = v_s/2$, which gives an estimate for v_s deviating only by about 0.6% from the exact result $\pi/2$. For the alternating-spin chain, similar fits give the numerical estimates $v_s = 0.38$, [1,1]=2.11, [2,0]=4.44, and [2,1]=5.69. In spite of the larger deviations from the theoretical results for $[m,n]$, the observed structure of the lowest-lying part of the spectrum in the alternating-spin model remains close to the structure in the reference spin-$\frac{1}{2}$ Heisenberg chain [32].

The established one-to-one mapping of the lowest-lying excitations of both models suggests similar critical properties. Since the unit cell of the reference spin-$\frac{1}{2}$ model contains two equivalent lattice sites, under PBC this means a doubling of the spectrum and, in particular, two equivalent critical modes. This explains the discussed doubling of the lowest-lying excitations in the alternating-spin $(1, \frac{1}{2})$ ring. Thus, both the GS entanglement entropy as well as the FSS properties of the SL phase point towards a Gaussian type critical behavior. Since the alternating-spin $(1, \frac{1}{2})$ ring exhibits two equivalent critical modes, the SL state may be interpreted as a critical spin-liquid phase described by two Gaussian conformal theories associated with these modes. Similar critical phases have been studied in some exactly solvable models, including spin models with extra three-body exchange interactions. In particular, there is an exactly-solvable alternating-spin (S,σ) model [33, 34] closely related to the generic model discussed in

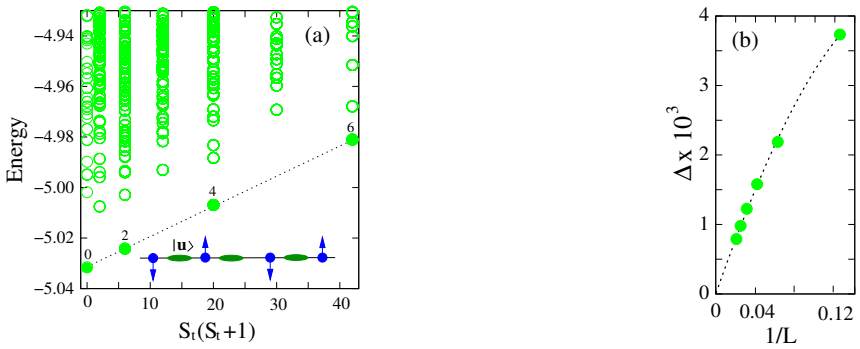

Figure 5. (a) Numerical ED results for the energy spectrum of the alternating-spin ($S = 1$, $\sigma = \frac{1}{2}$) ring ($L = 8$, $t = 110°$) *vs* $S_t(S_t + 1)$, where S_t is the total spin. The lowest multiplets in the even S_t sectors (filled circles) form a tower of states with energies $E(S) \propto S_t(S_t + 1)$. The dashed line is a guide for the eye. Inset: Cartoon of the suggested nematic-like state in the N sector. The ellipses denote the local nematic states $|\boldsymbol{u}\rangle = \sum_\alpha u^\alpha |\alpha\rangle$, where $\boldsymbol{u}$ is a unit real vector and $|\alpha\rangle$ ($\alpha = x, y, z$) is the vector basis of the spin-1 operator $\boldsymbol{S}$. (b) FSS of the lowest quintet gap ($t = 110°$, DMRG, OBC). The dashed line shows the optimal fitting ansatz $\Delta(L) = a_0 + a_1/L + a_2/L^2$.

this work at the point $t = 45°$. In fact, the difference between both models is reduced to an additional FM exchange term ($h_n^{\sigma\sigma} = J_3 \boldsymbol{\sigma}_{2n-1} \cdot \boldsymbol{\sigma}_{2n+1}$, $J_3 < 0$) in the exactly solvable model. Assuming that $h_n^{\sigma\sigma}$ represents an irrelevant operator (in a renormalization group sense), it may be speculated that both models exhibit similar critical properties. In particular, for the exactly solvable (S, σ) model, it has been predicted [33] that the critical behavior can be described by an effective central charge which is the sum of the central charges related with two critical modes, t.e., $c_{eff} = 3\sigma/(\sigma + 1) + 3(S - \sigma)/(S - \sigma + 1)$. In the special case $(S, \sigma) = (1, \frac{1}{2})$ this gives $c_{eff} = 1 + 1 = 2$, which coincides with the expected critical behavior of the SL phase.

4. Nematic-like phase (N)

The numerical ED results for the low-lying excitations in the periodic $L = 8$ chain, figure (1), point towards a different non-magnetic GS in the interval $\frac{\pi}{2} \lesssim t \lesssim \frac{2\pi}{3}$. Indeed, in the vicinity of $t = \frac{\pi}{2}$ the lowest quintet excitation is strongly softened and becomes the first excited state up to $t \simeq \frac{2\pi}{3}$. DMRG results for somewhat larger periodic systems (up to $L = 28$) confirm the picture with a lowest quintet excitation [35]. Further information about the non-magnetic state can be extracted form figure 5, showing ED results for the excitation spectrum of the same system at $t = 110°$ in different total-spin (S_t) sectors. An obvious feature of the presented spectrum is the established tower of well-separated lowest multiplets containing only even S_t sectors. Furthermore, the energies in the tower scale as $E(S) \propto S_t(S_t + 1)$. The observed structure is known as a fingerprint of the spin quadrupolar (i.e., nematic) order [36], unlike the Anderson tower – a characteristic of the Néel order – containing all S_t sectors [37]. In fact, Anderson towers of states have been observed even in some finite isotropic spin-S chains and magnetic molecules [38, 39, 40], including spin-$\frac{1}{2}$ Heisenberg chains [41]. In the same spirit, we consider the specific structure in figure 5a as a fingerprint of a non-magnetic state with dominant quadrupolar spin fluctuations. The FSS of the quintet excitation gap $\Delta(L) \propto 1/L$, figure 5b, pointing towards a gapless N state, is consistent with the above suggestion. Finally, in the Inset of figure 5a we show the cartoon of a tentative nematic-like state built from the on-site nematic states $|\boldsymbol{u}\rangle$ of the spin-1 operators, which respects both the established structure of the spectrum as well as the DMRG data implying extremely weak nearest-neighbor $S\sigma$ correlations

($|\langle \boldsymbol{S}_{2n} \cdot \boldsymbol{\sigma}_{2n\pm1} \rangle| < 0.07$) in the whole region occupied by the N phase.

5. Conclusion

It is worth emphasizing that the establishment of the discussed states is directly related to some peculiarities of the dominating three-body interaction such as the maintenance of collinear classical states and the promotion of nearest-neighbor spin clustering. As with the bilinear interaction in Eq. (1), in the N phase ($J_1 < 0$) its role is to weaken the AFM nearest-neighbor $S\sigma$ correlations, while in the SL phase ($J_1 > 0$) it enhances the tendency towards the formation of spin $(S - \sigma)$ states of the neighboring spins $\boldsymbol{S}_{2n} + \sigma_{2n\pm1}$. In this sense, an analogue of the SL state in spin-S AFM chains with extra three-body terms is the recently predicted fully-dimerized (Majumdar-Ghosh type) GS [11]. Obviously, the alternating-spin systems suggest more variety in this direction. Finally, it may be expected that most of discussed effects of the three-body exchange interaction persist in higher space dimensions. We believe that the presented results will encourage future search for real systems with pronounced three-body exchange effects.

Acknowledgments

We are grateful to Jörg Ummethum for adapting his DMRG code [42, 43] to three-body exchange interactions. N.B.I. thanks Bielefeld University for its hospitality. This research was supported by the Deutsche Forschungsgemeinschaft (SCHN 615/20-1), Deutscher Academischer Austausch Dienst (Grant PPP Bulgarien 57085392), and the National Science Foundation of Bulgaria [Grant DNTS/Germany/01/2 (03.09.2014)].

References

[1] Lhuillier C and Misguich G, *Introduction to frustrated magnetism Materials, Experiments, Theory* 2011 (Springer Series in Solid State Sciences vol 164) ed C Lacroix, P Mendels and F Mila (Berlin Heidelberg: Springer Verlag) chapter 2 pp 23-41
[2] see, e.g., Läuchli A, Schmid G and Trebst S 2006 *Phys. Rev.* B **74**144426, and references therein.
[3] Harada K and Kawashima 2002, *Phys. Rev.* B **65** 052403
[4] Tóth T A, Läuchli A M, Mila F and Penc K 2012 *Phys. Rev.* B **85** 140403(R)
[5] Momoi T, Sindzingre P and Shannon N 2006 *Phys. Rev. Lett.* **97** 257204
[6] Smerald A and Shannon N 2013 *Phys. Rev.* B **88** 184430
[7] Andrei N and Johannesson H 1984 *Phys. Lett.* A **100** 108
[8] de Vega H J and Woynarovich F 1992 *J. Phys. A: Math. Gen.* **25** 4499
[9] de Vega H J, Mezincescu L and Nepomechie R I 1994 *Phys. Rev.* B **49**, 13223
[10] Ribeiro G A P and Klümper A 2008 *Nucl. Phys.* B **801** [FS] 247
[11] Michaud F, Vernay F , Manmana S R and Mila F 2012 *Phys. Rev. Lett.* **108** 127202
[12] Michaud F, Manmana S R and Mila F 2013 *Phys. Rev.* B **87** 140404(R)
[13] Michaud F and Mila F 2013 *Phys. Rev.* B **88** 094435
[14] Wang Z -Y, Furuya S C, Nakamura M and Komakura R 2013 *Phys. Rev.* B **88** 224419
[15] Falk U, Furrer A, Güdel H U and Kjems J K 1986 *Phys. Rev. Lett.* **56** 1956
[16] Falk U, Furrer A, Kjems J K and Güdel H U 1984 *Phys. Rev. Lett.* **52** 1336
[17] Pachos J K and Plenio M B 2004 *Phys. Rev. Lett.* **93** 056402
[18] As the formation of local nearest-neighbor singlet dimer states is excluded in the alternating-spin systems, one may expect a different impact of the extra three-body terms as compared to the uniform-spin Heisenberg models.
[19] Furrer A 2010 *Int. J. Mod. Phys.* B **24** 3653
[20] Furrer A and Waldmann O 2013 *Rev. Mod. Phys.* **85** 367
[21] Landee Ch P and Turnbull M M 2013 *Eur. J. Inorg. Chem.* **2013** 2266
[22] In the extreme quantum case ($S = 1$, $\sigma = \frac{1}{2}$), $\mathcal{H}_{\sigma S}$ reproduces (up to irrelevant terms) the effective Hamiltonian of an isotropic spin-$\frac{1}{2}$ diamond chain with ring interactions in the subspace where any pair of "up" and "down" plaquette spins is in a triplet state.
[23] Ivanov N B, Richter J and Schulenburg J 2009 *Phys. Rev.* B **79** 104412
[24] Ivanov N B 2009 Condensed Matter Physics **12** 435
[25] Ivanov N B Ummethum J and Schnack J (to be published)
[26] Holzhey C, Larsen F and Wilczek F 1994 *Nucl. Phys.* B **424** 443

[27] Calabrese P and Cardy J 2004 *J. Stat. Mech.* **06** P06002
[28] Laflorencie N, Sørensen E S , Chang M S and Affleck I 2006 *Phys. Rev. Lett.* **96** 100603
[29] Alcaraz F C, Barber M N, Batchelor M T, Baxter R J and Quispel G R W 1987 *J. Math. Phys.* A **20** 6397
[30] Alcaraz F C, Berganza M I and Sierra G 2011 *Phys. Rev. Lett.* **106** 201601
[31] see, e.g., Hallberg K, Wang X q G, Horsch P and Moreo A 1996 *Phys. Rev. Lett.* **76** 4955, and references therein.
[32] As may be expected, in the middle of the range occupied by the SL phase, where the doubling of the lowest singlet and triplet states with L is faster (see figure 1), the deviations of $[m, n]$ from the theoretical results are smaller. For example, at $t = 63.4^\circ$ the same fitting procedure gives $v_s = 1.88$, $[1, 1] = 1.93$, $[2, 0] = 4.00$, and $[2, 1] = 5.35$.
[33] Aladim s R and Martins M J 1993 *J. Phys.* A **26** L529
[34] Bytsko A and Doikou A 2004 *J. Phys.* A **37** 4465
[35] Unfortunately, an extensive numerical analysis of the FSS properties of the excitation gaps is hampered by a slow convergence of the DMRG method in this region.
[36] see, e.g., Läuchli A, Domenge J C, Lhuillier C, Sindzingre P and Troyer M 2005 *Phys. Rev. Lett.* **95** 137206, and references therein.
[37] Anderson P W 1952 *Phys. Rev.* B **86** 694
[38] Schnack J and Luban M 2000 *Phys. Rev.* B **63** 014418
[39] Waldmann O 2001 *Phys. Rev.* B **65** 024424
[40] Machens A, Konstantinidis N P, Waldmann O, Schneider I and Eggert S 2013 *Phys. Rev.* B **87** 144409
[41] Eggert S and Affleck I 1992 *Phys. Rev.* B **46** 10866
[42] Ummethum J, Nehrkorn J, Mukherjee S, Ivanov N B, Stuiber S, Strassle Th, Tregenna-Piggott P L W, Mutka H, Christou G, Waldmann O and Schnack J 2012 *Phys. Rev.* B **86** 104403
[43] Schnack J and Ummethum J 2013 *Polyhedron* **66** 28